Generalized Volume-Surface Integral Equation for Modeling Inhomogeneities Within High Contrast Composite Structures

Brian C. Usner, *Student Member, IEEE*, Kubilay Sertel, *Member, IEEE*, Michael A. Carr, *Member, IEEE*, and John L. Volakis, *Fellow, IEEE*

***Abstract*—Numerical solutions of volume integral equations with high contrast inhomogeneous materials require extremely fine discretization rates making their utility very limited. Given the application of such materials for antennas and metamaterials, it is extremely important to explore computationally efficient modeling methods. In this paper, we propose a novel volume integral equation technique where the domain is divided into different material regions each represented by a corresponding uniform background medium coupled with a variation, together representing the overall inhomogeneity. This perturbational approach enables us to use different Green's functions for each material region. Hence, the resulting volume-surface integral equation alleviates the necessity for higher discretizations within the higher contrast regions. With the incorporation of a junction resolution algorithm for the surface integral equations defined on domain boundaries, we show that the proposed volume-surface integral equation formulation can be generalized to model arbitrary composite structures incorporating conducting bodies as well as highly inhomogeneous material regions.**

***Index Terms*—Hybrid methods, metamaterials, method of moments (MoM), surface integral equation (SIE), volume integral equation (VIE).**

I. Introduction

EFFECTIVE modeling of arbitrarily shaped inhomogeneous composite structures for scattering and radiation applications has received much attention within the last two decades. Methods based on a hybrid finite element-boundary integral (FE-BI) approach have been proposed to model such structures [1]–[4]. However, for high contrast materials (i.e., materials with large permittivity and/or permeability values), this hybrid approach becomes inefficient and can produce badly conditioned system matrices. Integral equation methods based on the Poggio, Miller, Chang, Harrington, Wu, Tsai (PMCHWT) formulation [5]–[7] are quite resilient in modeling high contrast materials since the homogeneous domain can be represented by the appropriate Green's function. However, because this SIE is applicable only to piecewise homogeneous media [8]–[14], modeling objects consisting of many regions of anisotropic and/or inhomogeneous material regions require a volume integral equation (VIE) approach [15]–[21]. As such, a combined volume-surface integral equation (VSIE) approach is required for modeling arbitrary inhomogeneous composite media.

When high-contrast materials are considered, the typical VIE formulation requires many unknowns leading to computationally intractable problems [22]. Though the VIE has been applied to structures consisting of high-contrast media [23], [24] the large number of unknowns needed to represent the highly varying field patterns within high-contrast media makes them unattractive. In contrast, as mentioned above, the SIE does not suffer from resolution issues in presence of high-contrast materials (especially when far-field information is required). In light of this, a VSIE incorporating a novel factorization of the material parameters is presented to alleviate the computational burden associated with VIE when varying high-contrast material parameters are considered. The proposed formulation invokes the VIE only over regions where the material is actually varying, and the SIE is employed elsewhere along the boundaries of the homogeneous (possibly high contrast) regions. Further, since the VIE is only used to account for material perturbations, there is a significant alleviation in the discretization rate. The proposed formulation, though similar in concept to that in [25], is unique in the sense that it can handle anisotropic materials through a proper choice of volume field unknowns and is void of ill conditioning problems due to large matrix entries for high contrast materials that are just slightly varying. Overall, the proposed formulation encapsulates all traditional VSIE formulations [26]–[30], including the PMCHWT and the usual VIE and SIE formulations. Therefore, we will refer to this new formulation as the *generalize* VSIE.

In the following, we begin by developing the generalized VSIE starting with a unique decomposition of the material parameters ε and μ. This is followed by the method of moments (MoM) solution using curvilinear hexahedral and quadrilateral finite elements. We note that the Petrov–Galerkin testing procedure [31] is applied to the VIE to yield a robust matrix system over curvilinear finite elements [32]. The matrix assembly process is implemented via a junction resolution algorithm that is similar to the implementations described in [13] and [14]. The final section presents results that validate the efficiency and accuracy of the formulation by considering scattering from three canonical structures.

Manuscript received June 13, 2005; revised September 9, 2005. This work was in part supported by the U.S. Air Force Office of Scientific Research Grant FA9550-04-1-0359 and under the NASA GSRP Fellowship program.

The authors are with the ElectroScience Laboratory, Department of Electrical Engineering, The Ohio State University, Columbus, OH 43212-1191 USA (e-mail: usner.2@osu.edu).

Digital Object Identifier 10.1109/TAP.2005.861579

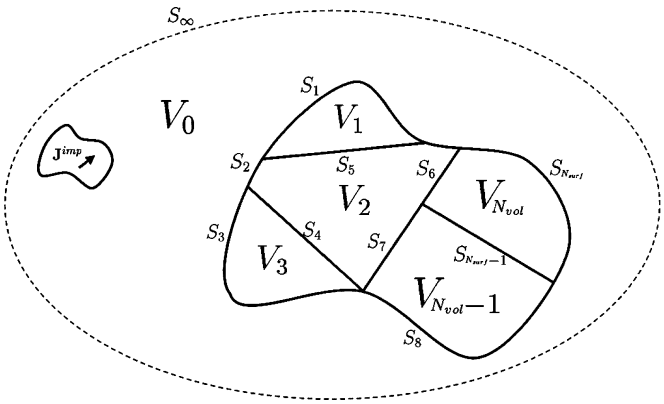

Fig. 1. Partitioning of space for the generalized VSIE.

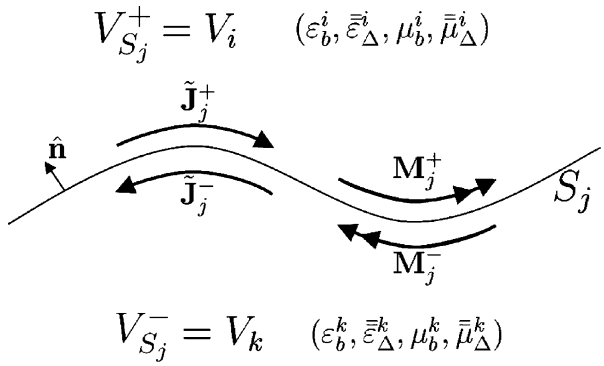

Fig. 2. Current relationships for the generalized VSIE.

II. Generalized VSIE Formulation

To describe the proposed generalized VSIE, we refer to Fig. 1 which shows several volume sections $(V_0, V_1, \ldots, V_{N_{\rm vol}})$, each associated with a different dielectric media which maybe associated either with a uniform or a varying material profile. Because of the latter, it is important to represent the relative permittivity in each of the volumes as

$$\bar{\bar{\varepsilon}}_r(\mathbf{r}) = \varepsilon_b \bar{\bar{I}} + \bar{\bar{\varepsilon}}_\delta(\mathbf{r}) = \varepsilon_b \left[\bar{\bar{I}} + \varepsilon_b^{-1}\bar{\bar{\varepsilon}}_\delta(\mathbf{r})\right] = \varepsilon_b \bar{\bar{\varepsilon}}_\Delta(\mathbf{r}) \quad (1)$$

in which $\bar{\bar{I}}$ is the identity dyadic. Similarly, the permeability $\bar{\bar{\mu}}_r$ can be written as

$$\bar{\bar{\mu}}_r(\mathbf{r}) = \mu_b \bar{\bar{I}} + \bar{\bar{\mu}}_\delta(\mathbf{r}) = \mu_b \left[\bar{\bar{I}} + \mu_b^{-1}\bar{\bar{\mu}}_\delta(\mathbf{r})\right] = \mu_b \bar{\bar{\mu}}_\Delta(\mathbf{r}). \quad (2)$$

Here, the uniform terms ε_b and μ_b constitute an equivalent background homogeneous region that can be varied by way of the modulation terms $\bar{\bar{\varepsilon}}_\Delta(\mathbf{r})$ and $\bar{\bar{\mu}}_\Delta(\mathbf{r})$. In what follows, we will see that it is these modulation terms that contribute to the equivalent sources within the generalized VSIE.

Referring to Fig. 1, we partition the entire volume V into $(N_{\rm vol}+1)$ volumes so that $V = \cup_{i=0}^{N_{\rm vol}} V_i$ and $V_i \cap V_j = \{\varnothing\}$ for $i \neq j$. Each volume V_i is characterized by the parameter set $\{\varepsilon_b^i, \bar{\bar{\varepsilon}}_\Delta^i, \mu_b^i, \bar{\bar{\mu}}_\Delta^i\}$ with the wavenumber k_i given by $k_i = k_0\sqrt{\varepsilon_b^i \mu_b^i}$. The volume V_0 is assumed here to be free space of wavenumber k_0. We denote the boundary surfaces defined by the adjoining volumes as S_j, $\{j = 1 \ldots N_{\rm surf}\}$, where the number of surfaces, $N_{\rm surf}$, depends on the topology of the partitioned volumes. The complete boundary surrounding V_i can be represented as $\partial V_i = \cup_{j\in\{p_i\}} S_j$, where the set $\{p_i\}$ contains the numbers of surfaces enclosing V_i. Since each surface S_j is a boundary formed by the junction of the volume pair $(V_{S_j}^+, V_{S_j}^-)$, where $V_{S_j}^\pm \in \{V_i\}$, we introduce the convenient symbolic function $\mathrm{sign}(i,j)$

$$\mathrm{sign}(i,j) = \begin{cases} + & \text{if } V_i = V_{S_j}^+ \\ - & \text{if } V_i = V_{S_j}^-. \end{cases} \quad (3)$$

Throughout the paper, we will also assume that all normals $\hat{n}$ on any surface S_j point in the direction of volume $V_{S_j}^+$.

To construct the integral equation(s) for each V_i, we begin with the time-harmonic vector wave equations (an $e^{j\omega t}$ time convention is assumed and suppressed throughout)

$$\nabla\times\nabla\times\mathbf{E}_i - k_i^2\mathbf{E}_i = -jk_0\mu_b^i\left(\tilde{\mathbf{J}}_{V_i}^{\rm eq} + \tilde{\mathbf{J}}_i^{\rm imp}\right) \quad (4)$$

$$\nabla\times\nabla\times\tilde{\mathbf{H}}_i - k_i^2\tilde{\mathbf{H}}_i = -jk_0\varepsilon_b^i\mathbf{M}_{V_i}^{\rm eq} + \nabla\times\left[\left(\bar{\bar{\varepsilon}}_\Delta^i\right)^{-1}\tilde{\mathbf{J}}_i^{\rm imp}\right] \quad (5)$$

in which $(\mathbf{E}_i, \tilde{\mathbf{H}}_i)$ represent the electric and augmented magnetic fields within the ith volume V_i, where the augmented magnetic field $\tilde{\mathbf{H}}_i$ is defined with respect to the free-space impedance Z_0, viz. $\tilde{\mathbf{H}}_i \triangleq Z_0\mathbf{H}_i$. Likewise, the augmented source $\tilde{\mathbf{J}}_i^{\rm imp} = Z_0\mathbf{J}_i^{\rm imp}$ represents any impressed currents within V_i. The wave equations (4) and (5) imply that the electric and magnetic field intensities can be attributed to the equivalent volume sources $\tilde{\mathbf{J}}_{V_i}^{\rm eq}$ and $\mathbf{M}_{V_i}^{\rm eq}$ given by

$$\tilde{\mathbf{J}}_{V_i}^{\rm eq} = jk_0\varepsilon_b^i\left(\bar{\bar{\varepsilon}}_\Delta^i - \bar{\bar{I}}\right)\mathbf{E}_i + \nabla\times\left[\left(\bar{\bar{\mu}}_\Delta^i - \bar{\bar{I}}\right)\tilde{\mathbf{H}}_i\right] \quad (6)$$

$$\mathbf{M}_{V_i}^{\rm eq} = jk_0\mu_b^i\left(\bar{\bar{\mu}}_\Delta^i - \bar{\bar{I}}\right)\tilde{\mathbf{H}}_i - \nabla\times\left[\left(\bar{\bar{\varepsilon}}_\Delta^i - \bar{\bar{I}}\right)\mathbf{E}_i\right]. \quad (7)$$

In addition to these volume currents, we may also define equivalent surface currents attributed to material discontinuities at the surfaces bounding the volumes $\{V_i\}$. These currents are given by

$$\tilde{\mathbf{J}}_j^\pm = \pm\hat{n}\times\tilde{\mathbf{H}}_j^\pm \quad \text{and} \quad \mathbf{M}_j^\pm = \mp\hat{n}\times\mathbf{E}_j^\pm \quad (8)$$

where the index j implies that these currents are located at the jth surface S_j (see Fig. 2). It should be also noted that within the ith volume surrounded (in part) by the surface S_j, the following expressions hold:

$$\tilde{\mathbf{J}}_j^{{\rm sign}(i,j)} = \mathrm{sign}(i,j)(\hat{n}\times\tilde{\mathbf{H}}_i) \quad (9)$$

$$\mathbf{M}_j^{{\rm sign}(i,j)} = -\mathrm{sign}(i,j)(\hat{n}\times\mathbf{E}_i). \quad (10)$$

Employing the above conventions, we can express the scattered field attributed to the volume V_i as

$$\begin{aligned}\mathbf{E}_i^{\rm scat}(\mathbf{r}) = {} & k_i^2 \int_{V_i} dr' \bar{\bar{G}}_{k_i} \cdot \left(\bar{\bar{\varepsilon}}_\Delta^i - \bar{\bar{I}}\right) \mathbf{E}_i \\ & + jk_0\mu_b^i \int_{V_i} dr' \nabla' g_{k_i} \times \left[\left(\bar{\bar{\mu}}_\Delta^i - \bar{\bar{I}}\right) \tilde{\mathbf{H}}_i\right] \\ & - jk_0\mu_b^i \sum_{j=\{p_i\}} \int_{S_j} dr' \bar{\bar{G}}_{k_i} \cdot \tilde{\mathbf{J}}_j^{{\rm sign}(i,j)} \\ & + \sum_{j=\{p_i\}} \int_{S_j} dr' \nabla' g_{k_i} \times \mathbf{M}_j^{{\rm sign}(i,j)} \end{aligned} \tag{11}$$

where the dyadic Green's function is defined as $\bar{\bar{G}}_{k_i}(\mathbf{r},\mathbf{r}') = [\bar{\bar{I}} + (1/k_i^2)\nabla\nabla] g_{k_i}(\mathbf{r},\mathbf{r}')$, with $g_{k_i}(\mathbf{r},\mathbf{r}') = e^{-jk_i|\mathbf{r}-\mathbf{r}'|}/(4\pi|\mathbf{r}-\mathbf{r}'|)$ and $k_i = k_0\sqrt{\varepsilon_b^i\mu_b^i}$, which refers to the wavenumber of the ith material volume comprising the domain. The dual of (11) is

$$\begin{aligned}\tilde{\mathbf{H}}_i^{\rm scat}(\mathbf{r}) = {} & k_i^2 \int_{V_i} dr' \bar{\bar{G}}_{k_i} \cdot \left(\bar{\bar{\mu}}_\Delta^i - \bar{\bar{I}}\right) \tilde{\mathbf{H}}_i \\ & - jk_0\varepsilon_b^i \int_{V_i} dr' \nabla' g_{k_i} \times \left[\left(\bar{\bar{\varepsilon}}_\Delta^i - \bar{\bar{I}}\right) \mathbf{E}_i\right] \\ & - jk_0\varepsilon_b^i \sum_{j=\{p_i\}} \int_{S_j} dr' \bar{\bar{G}}_{k_i} \cdot \mathbf{M}_j^{{\rm sign}(i,j)} \\ & - \sum_{j=\{p_i\}} \int_{S_j} dr' \nabla' g_{k_i} \times \tilde{\mathbf{J}}_j^{{\rm sign}(i,j)}. \end{aligned} \tag{12}$$

Note that these expressions contain the contributions from the surface equivalent currents enclosing V_i as well as those due to the volume currents attributed to the variations ($\bar{\bar{\varepsilon}}_\Delta^i$, $\bar{\bar{\mu}}_\Delta^i$) of the parameters (ε_b^i, μ_b^i). Having expressions (11) and its dual (12), we next proceed to set up the appropriate integral equations to solve for ($\tilde{\mathbf{J}}$, $\mathbf{M}$) on the boundaries and $\mathbf{E}$ within the volumes ($\tilde{\mathbf{H}}$ is an unknown only if $\bar{\bar{\mu}}_\Delta^i \neq \bar{\bar{I}}$). Proceeding to do so, the integral equations take the form

$$\mathbf{E}_i - \mathbf{E}_i^{\rm scat} = \mathbf{E}^{\rm inc}\delta_i, \quad \mathbf{r} \in V_i \tag{13}$$

$$\gamma_t\mathbf{E}_i - \gamma_t\mathbf{E}_i^{\rm scat} = \gamma_t\mathbf{E}^{\rm inc}\delta_i, \quad \mathbf{r} \in \partial V_i \tag{14}$$

$$\gamma_t\tilde{\mathbf{H}}_i - \gamma_t\tilde{\mathbf{H}}_i^{\rm scat} = \gamma_t\tilde{\mathbf{H}}^{\rm inc}\delta_i, \quad \mathbf{r} \in \partial V_i \tag{15}$$

where γ_t is the tangential surface trace operator used in [33]. Note that the excitations ($\mathbf{E}^{\rm inc}$, $\tilde{\mathbf{H}}^{\rm inc}$) are generated from $\tilde{\mathbf{J}}_i^{\rm imp}$ located within V_0 and the Kronecker delta function δ_i is used to imply that the source only excites those equivalent currents radiating within V_0. In addition, the expressions in (9) and (10) can be used to replace $\gamma_t\mathbf{E}_i$ and $\gamma_t\tilde{\mathbf{H}}_i$ with ${\rm sign}(i,j)\hat{n} \times \mathbf{M}_j^{{\rm sign}(i,j)}$ and $-{\rm sign}(i,j)\hat{n} \times \tilde{\mathbf{J}}_j^{{\rm sign}(i,j)}$, respectively. It should be noted that (13)–(15) need be enforced for all volumes V_i with the resulting equations being condensed by enforcing field continuity and boundary conditions to generate the matrix system.

In order to elucidate the formulation's ability to handle inhomogeneities inside high contrast medium, we consider here, without loss of generality, the scattered electric field due to the equivalent volume currents arising from varying permittivities

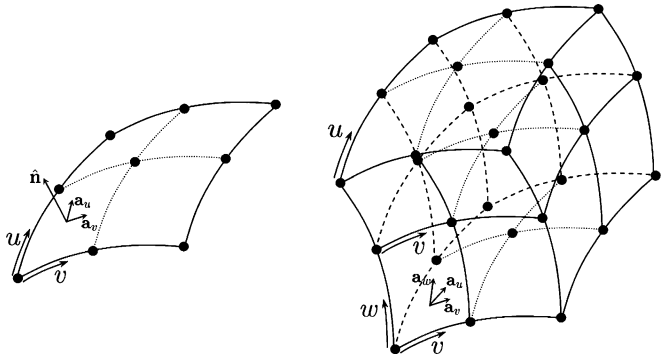

Fig. 3. Curvilinear finite-elements used for discretization.

(note: similar arguments can be made for other volume current kernels within the formulation). In typical VIE formulations, the scattered field is given by $\mathbf{E}^{\rm scat} = k_0^2 \int_V dr' \bar{\bar{G}}_{k_0} \cdot (\bar{\bar{\varepsilon}}_r - \bar{\bar{I}})\mathbf{E}$. Notice that as $|\bar{\bar{\varepsilon}}_r|$ becomes large so does the scattered field kernel. In contrast, the corresponding scattered field kernel in (11) is a perturbation term whose magnitude is dictated more by the size of $|\bar{\bar{\varepsilon}}_r - \varepsilon_b\bar{\bar{I}}|$. Thus the contribution of this kernel is dictated less by the high contrast of the material but by the severity of inhomogeneity or anisotropy. In addition, by virtue of the boundary integral around the material region, the Green's function can be chosen to be more closely matched to the actual phase propagation within the material region.

III. MoM Implementation

To solve the system in (13)–(15) numerically, discretization is carried out using 9-node curvilinear quadrilateral and 27-node curvilinear hexahedral finite elements (see Fig. 3), similar to those used in [4] and [34]. Specifically, the surfaces $\{S_j\}$ are discretized using the surface quads shown to the left of Fig. 3, whereas the field within the volumes $\{V_i\}$ is discretized using the hexahedra shown to the right of Fig. 3.

The surface currents on S_j are then expressed as (see Figs. 2 and 3)

$$\tilde{\mathbf{J}}_j^{\pm}(\mathbf{r}) \simeq \sum_{n=1}^{N_{\rm quad}^j} \sum_{p=1}^{4} J_{np}^{\pm,j} \mathbf{f}_p\left(\mathbf{r}_n(u,v)\right) \tag{16}$$

$$\mathbf{M}_j^{\pm}(\mathbf{r}) \simeq \sum_{n=1}^{N_{\rm quad}^j} \sum_{p=1}^{4} M_{np}^{\pm,j} \mathbf{f}_p\left(\mathbf{r}_n(u,v)\right) \tag{17}$$

where $J_{np}^{\pm,j}$ and $M_{np}^{\pm,j}$ are the current values corresponding to the pth local edge of each element comprising the surface S_j. The basis functions $\{\mathbf{f}_p\}$ are the divergence-conforming roof-top functions defined in the parametric space [4]. These allow for normal field continuity across element edges.

The electric field intensity within V_i is expressed as

$$\mathbf{E}_i(\mathbf{r}) \simeq \sum_{n=1}^{N_{\rm hex}^i} \sum_{p=1}^{12} E_{np}^i \mathbf{h}_p\left(\mathbf{r}_n(u,v,w)\right) \tag{18}$$

where E_{np}^i denote the field values corresponding to the pth local edge belonging to the nth hexahedral element comprising the volume V_i. The basis functions $\{\mathbf{h}_p\}$ are the curl-conforming parametric edge basis functions discussed in [4], [32]. These

allow for explicit enforcement of tangential field continuity across element faces.

As usual, the MoM system is developed by substituting the current and field expansions (16)–(18) into the integral equations implied by (13)–(15). The volume integral equation (13) is then tested within the V_i volumes having $\bar{\bar{\varepsilon}}_\Delta \neq \bar{\bar{I}}$, where the testing functions proposed in [32] are employed. These testing functions satisfy the Petrov–Galerkin requirements for the second-kind integral equations [31] and were shown necessary to achieve well conditioned systems and accurate solutions. Typical Galerkin's testing is employed for the surface integral equations (14) and (15) bounding the volumes V_i. After carefully carrying out the matrix assembly process (enforcing field continuity at the common volume boundaries), we get the MoM system

$$\begin{bmatrix} \bar{\mathbf{Z}}^{EE} & \bar{\mathbf{Z}}^{EM} & \bar{\mathbf{Z}}^{EJ} \\ \bar{\mathbf{Z}}^{ME} & \bar{\mathbf{Z}}^{MM} & \bar{\mathbf{Z}}^{MJ} \\ \bar{\mathbf{Z}}^{JE} & \bar{\mathbf{Z}}^{JM} & \bar{\mathbf{Z}}^{JJ} \end{bmatrix} \begin{bmatrix} \mathbf{E} \\ \mathbf{M} \\ \mathbf{J} \end{bmatrix} = \begin{bmatrix} \mathbf{b}^E \\ \mathbf{b}^M \\ \mathbf{b}^J \end{bmatrix}. \quad (19)$$

As described previously in [11], [13] and [14], the matrix elements within the MoM blocks in (19) are filled using elements of the local matrices constructed through element-to-element testing (explicit expressions of which can be found in Appendix I). For the surface currents, this mapping is described by a junction resolution algorithm that relates the local currents defined in (16) and (17) to the global currents. Likewise, for the electric field unknowns, this mapping implies explicit enforcement of tangential field continuity across the hexahedral element faces. We remark here that the magnetic surface current unknowns could be paired with their corresponding electric field unknowns through the relationship given in (8), thus, reducing the total number of unknowns. However, no such pairing is enforced in this work. In addition, as is well known for the PMCHWT formulation, the SIEs in the lower two rows in (19) is void of internal resonances as long as no partitioned volume region is completely enclosed by either a PEC or PMC surface. For such cases, a combined field integral equation (CFIE) as described in [35] should be used. A CFIE version of (19), although straight forward to derive is not given in this paper since the need only arises when closed PEC/PMC bodies are present in the solution domain.

IV. Validations

A. Sphere Embedded in a Sphere

In our first example, we consider the geometry of Fig. 4. This is a high contrast dielectric sphere of radius $r = 0.1\lambda$ and $\varepsilon_r = 20$ embedded in a larger dielectric sphere of radius $r = 0.5\lambda$ and $\varepsilon_r = 10$. Our VSIE assumes an $\varepsilon_b = 10$ with $\varepsilon_\Delta = 2$ in the regions where $\varepsilon_r = 20$. To demostrate the applicability of our method, the volume integral in (13) is only invoked inside the smaller embedded sphere instead of the entire scattering domain. In Fig. 4 we present results for two cases: Case 1: the smaller dielectric sphere is concentric to the larger sphere and Case 2: the smaller dilectric sphere is translated 0.1λ in both the x- and y-directions. As seen, the first case compares well with the Mie series solution, whereas Case 2 demonstrates the formulations effectiveness to model field variations among displaced inclusions (a capability well suited for inverse scattering applications).

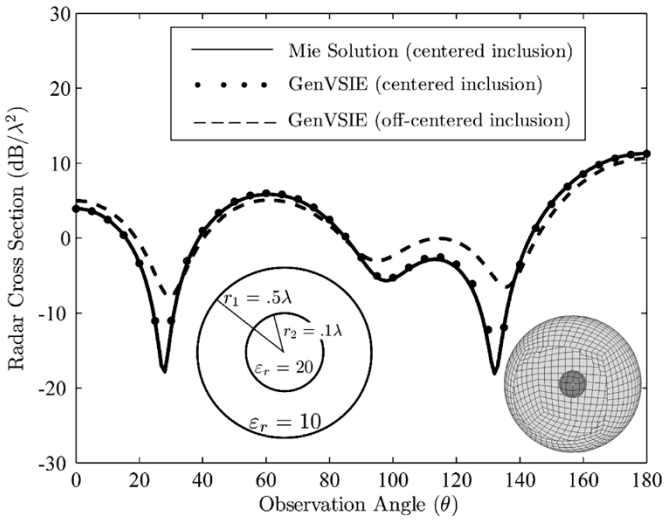

Fig. 4. Bistatic RCS (θ-cut, E_θ-polarization, $\mathbf{k}_{\rm inc} = -k_z$) of a dielectric sphere with $r = 0.1\lambda$ and $\varepsilon_r = 20$ embedded in a dielectric sphere with $r = 0.5\lambda$ and $\varepsilon_r = 10$. One result is shown for a centered inclusion (compared to Mie solution) and another result is shown for an off-centered inclusion (dashed line), where a change in scattered field is seen that demonstrates possible inverse scattering applications.

We remark that the discretization of the electric field within the VIE portion of the formulation was carried out using elements of average edge length equal to $\lambda/10$ instead of the typical $\lambda/40$ required by the contrast of the materials used in this example. As a result, we only needed 144 volume field unknowns and 5400 surface current unknowns to accurately solve the system. By comparison, if the usual VIE was to be used throughout the entire scattering domain, the dielectric contrasts would require approximately 64,000 volume elements requiring approximately 200 000 volume unknowns. We note that a similar number of unknowns would be required using the usual FE-BI formulation. Because of the much smaller number of unknowns needed for the proposed formulation, it is attractive for inverse scattering applications where one is searching for high contrast inclusions embedded within large material regions. Such problems are often encountered in biomedical microwave imaging applications [36].

B. Coated Ogive

We next consider a coated Ogive which is an elongated body of revolution, commonly used as a validation target in CEM [29]. Here, the coated Ogive has a length 2λ, a base radius of 0.24λ, and a coating of thickness 0.07λ, with $\varepsilon_r = 2.56 - j0.5$. We can of course chose to model the dielectric coating using the usual VSIE or the PMCHWT method. However, to demonstrate the robustness of the VSIE formulation, we arbitrarily chose ε_Δ to be $1 + j1$ corresponding to the factorization

$$\begin{aligned} \varepsilon_r &= (1.03 - j1.53) + (1.53 + j1.03) \\ &= (1.03 - j1.53)(1 + j1) = \varepsilon_b \varepsilon_\Delta. \end{aligned} \quad (20)$$

Fig. 5(a) compares results from the generalized VSIE and those from [29]. It can be seen from Fig. 5(a) that with the selected complex ε_Δ, our formulation compares well with the PMCHWT method and the VSIE results given in [29]. For clarity, the factorization presented in (20) corresponds to a homogeneous material coating with $\varepsilon_b = 1.03 - j1.53$ modulated by the vari-

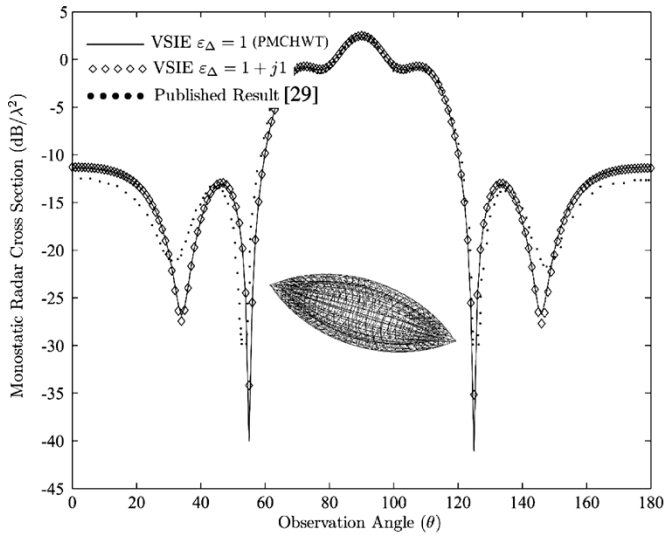

(a)

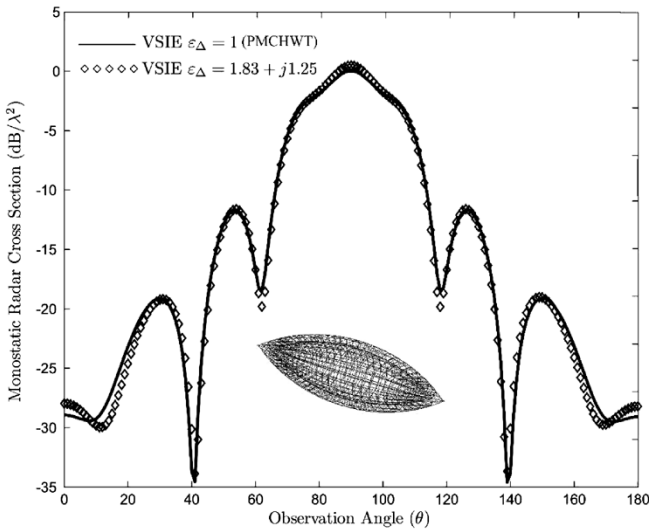

(b)

Fig. 5. Mono-static RCS of coated ogives. (a) Coated Ogive considered in [29] and (b) high contrast coated Ogive.

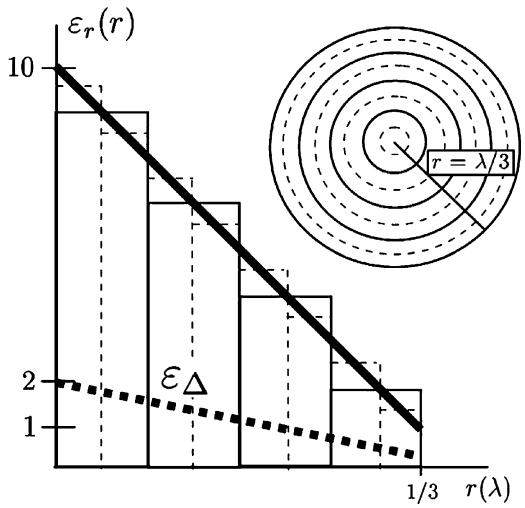

Fig. 6. Material profile for the smoothly varying inhomogeneous sphere of radius $r = \lambda/3$. Also shown is the material profile of the perturbation, $\varepsilon_\Delta(\mathbf{r})$, for an $\varepsilon_b = 5$, along with the staircase approximation to the material profile for the 4 and 8 layered sphere used within the PMCHWT implementation.

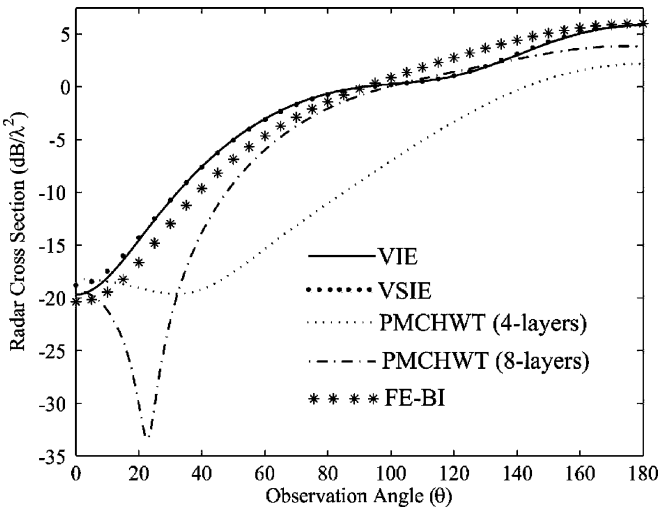

Fig. 7. Bistatic RCS (θ-cut, E_θ-polarization, $\mathbf{k}_{\rm inc} = -k_z$) of the smoothly varying inhomogeneous sphere depicted in Fig. 6.

ation $\varepsilon_\Delta = 1 + j1$ so as to represent a material having an $\varepsilon_r = 2.56 - j0.5$. Notice, also, that the chosen background medium in (20) is lossy. This choice ensures that the solution remains numerically stable (i.e., no gain within the material), leading to a well conditioned matrix systems.

To further demonstrate the robustness of our method, a higher contrast material is presented in Fig. 5(b) where the permittivity of the Ogive coating is increased to $\varepsilon_r = 17.97 - j14.57$. This coating will be modeled using a background $\varepsilon_b = 3.00 - j10.0$ and a variation $\varepsilon_\Delta = 1.83 + j1.25$ viz.

$$\begin{aligned}\varepsilon_r &= (3.00 - j10.0) + (14.97 - j4.57) \\ &= (3.00 - j10.0)(1.83 + j1.25) = \varepsilon_b \varepsilon_\Delta. \end{aligned} \tag{21}$$

Again, the background medium is selected to be lossy. The results are compared to the PMCHWT $(\varepsilon_\Delta = 1)$ implementation. As shown in Fig. 5(b), we have an excellent agreement even down to low RCS values. It is important to further note that although the contrast of the coating was increased, the same discretization density was used for the low and high contrast examples. Since design applications often seek material profiles (i.e., ε_Δ) that optimize a desired performance parameter, the presented results suggest that this VSIE is well suited in design applications utilizing high contrast material coatings.

C. Smoothly Varying Inhomogeneity

In the last example, we consider the scattering from a dielectric sphere of radius $r = \lambda/3$ having a material profile that varies radially (see Fig. 6) as

$$\varepsilon_r(r) = 10 - 27r \tag{22}$$

where r has units in terms of λ. To demonstrate the VSIE's capability to model smoothly varying material profiles, we select a background medium of $\varepsilon_b = 5$, for which $\varepsilon_\Delta(\mathbf{r}) = 2 - 5.4r$. In Fig. 7 we compare the VSIE result with that of the typical VIE solution as well as an FE-BI solution. In addition, we also incorporate a PMCHWT implementation of the inhomogeneous sphere using the layered sphere approximation with 4 and 8 concentric layers of constant dielectric. As seen in Fig. 7, the

VSIE result which required 882 VIE unknowns and 864 SIE unknowns compares well with that of the VIE result which required 1944 unknowns. Although the savings in the number of unknowns is not very significant, the reduction in the number of VIE unknowns drastically reduces the matrix fill time for the MoM system. Interestingly, we note that the results for both the 4 and 8 layered spheres are substantially different from each other and from the VIE, VSIE, and FE-BI result. This is entirely due to the approximation error introduced in modeling the smoothly varying material profile with uniform layers. For such a staircase approximation to be valid, one would need many such layers, which in turn could increase the computational cost of the PMCHWT formulation. For completeness, we used an FE-BI system of 6084 unknowns (with 1728 BI unknowns). Thus, because the 4 layered solution required 2400 unknowns and the 8 layered solution required 6000 unknowns, we can also claim that layered approximations of inhomogeneous materials may not always be the most efficient approach.

V. Conclusion

A generalized VSIE was proposed for modeling inhomogeneous volumes within high contrast composite materials. The advantage of this formulation is that the VIE is only invoked within regions where the material is actually varying. Concurrently, SIEs are employed at the boundaries of discontinuous volume regions where Green's functions for the high contrast background medium are used. The new VSIE leads to fewer unknowns making it useful in design or inverse scattering applications.

Appendix I
Element-to-Element Evaluations

The submatrices $\bar{\mathbf{Z}}^{EE}$, $\bar{\mathbf{Z}}^{EM}$, $\bar{\mathbf{Z}}^{EJ}$, $\bar{\mathbf{Z}}^{ME}$, $\bar{\mathbf{Z}}^{MM}$, $\bar{\mathbf{Z}}^{MJ}$, $\bar{\mathbf{Z}}^{JE}$, $\bar{\mathbf{Z}}^{JM}$, and $\bar{\mathbf{Z}}^{JJ}$ consist of a linear combination of values resulting from the element-to-element testing throughout the computational domain. As mentioned, this linear combination is dictated by the resolution algorithm linking the elemental (local) unknowns to the system (global) unknowns. It should be noted that testing only occurs between elements containing equivalent currents (volume or surface) that radiate within the same volume. Explicitly, the entries in the MoM submatrices consist of values found from the following expressions:

$$Z_{mn}^{EE} = \int_{\Omega_m^V} dr \mathbf{h}_m' \cdot \mathbf{h}_n - k_n^2 \int_{\Omega_m^V} dr \mathbf{h}_m' \cdot \int_{\Omega_n^V} dr' g_{k_n} (\bar{\bar{\varepsilon}}_\Delta - \bar{\bar{I}}) \mathbf{h}_n + \oint_{\Omega_m^V} dr\, (\hat{n} \cdot \mathbf{h}_m') \int_{\Omega_n^V} dr' \nabla' g_{k_n} \cdot (\bar{\bar{\varepsilon}}_\Delta - \bar{\bar{I}}) \mathbf{h}_n \tag{23}$$

$$Z_{mn}^{EM} = \int_{\Omega_m^V} dr \mathbf{h}_m' \cdot \int_{\Omega_n^S} dr' \nabla' g_{k_n} \times \mathbf{f}_n \tag{24}$$

$$Z_{mn}^{EJ} = jk_0 \mu_b^n \int_{\Omega_m^V} dr \mathbf{h}_m' \cdot \int_{\Omega_n^S} dr' g_{k_n} \mathbf{f}_n + \frac{j}{k_0 \varepsilon_b^n} \oint_{\Omega_m^V} dr\, (\hat{n} \cdot \mathbf{h}_m') \int_{\Omega_n^S} dr' g_{k_n} (\nabla' \cdot \mathbf{f}_n) \tag{25}$$

$$Z_{mn}^{ME} = jk_0 \varepsilon_b^n \int_{\Omega_m^S} dr \mathbf{f}_m \cdot \int_{\Omega_n^V} dr' \nabla' g_{k_n} \times \left[(\bar{\bar{\varepsilon}}_\Delta - \bar{\bar{I}}) \mathbf{h}_n \right] \tag{26}$$

$$Z_{mn}^{MM} = jk_0 \varepsilon_b^n \int_{\Omega_m^S} dr \mathbf{f}_m \cdot \int_{\Omega_n^S} dr' g_{k_n} \mathbf{f}_n - \frac{j}{k_0 \mu_b^n} \int_{\Omega_m^S} dr (\nabla \cdot \mathbf{f}_m) \int_{\Omega_n^S} dr' g_{k_n} (\nabla' \cdot \mathbf{f}_n) \tag{27}$$

$$Z_{mn}^{MJ} = -\frac{1}{2} \int_{\Omega_m^S} dr \mathbf{f}_m \cdot (\hat{n} \times \mathbf{f}_n) + \int_{\Omega_m^S} dr \mathbf{f}_m \cdot \oint_{\Omega_n^S} dr' \nabla' g_{k_n} \times \mathbf{f}_n \tag{28}$$

$$Z_{mn}^{JE} = -k_n^2 \int_{\Omega_m^S} dr \mathbf{f}_m \cdot \int_{\Omega_n^V} dr' g_{k_n} (\bar{\bar{\varepsilon}}_\Delta - \bar{\bar{I}}) \mathbf{h}_n - \int_{\Omega_m^S} dr (\nabla' \cdot \mathbf{f}_m) \int_{\Omega_n^V} dr' \nabla' g_{k_n} \cdot (\bar{\bar{\varepsilon}}_\Delta - \bar{\bar{I}}) \mathbf{h}_n \tag{29}$$

$$Z_{mn}^{JM} = -Z_{mn}^{MJ} \tag{30}$$

$$Z_{mn}^{JJ} = \frac{\mu_b^n}{\varepsilon_b^n} Z_{mn}^{MM}. \tag{31}$$

The excitation column entries contain linear combination of the following integrals:

$$b_m^E = \int_{\Omega_m^V \cap V_0} dr \mathbf{h}_m' \cdot \mathbf{E}^{\text{inc}} \tag{32}$$

$$b_m^M = \int_{\Omega_m^S \cap V_0} dr \mathbf{f}_m \cdot \tilde{\mathbf{H}}^{\text{inc}} \tag{33}$$

$$b_m^J = \int_{\Omega_m^S \cap V_0} dr \mathbf{f}_m \cdot \mathbf{E}^{\text{inc}}. \tag{34}$$

The elemental surface basis functions denoted here as $\mathbf{f}_n$ and having domain Ω_n^S are precisely those described in (16) and (17). Likewise, the elemental volume basis functions denoted here as $\mathbf{h}_n$ and having domain Ω_n^V are those described in (18). However, the testing functions $\mathbf{h}_n'$ are of the type described in [32]. The material parameters μ_b^n, ε_b^n, and k_n are those associated with the volume in which testing occurs.

Acknowledgment

The authors would like to thank Dr. M. D. Deshpande and the NASA GSRP fellowship program for their generous support throughout this work. In addition, the authors thank the reviewers for their helpful comments.

References

[1] X. Yuan, "Three dimensional electromagnetic scattering from inhomogeneous objects by the hybrid moment and finite element method," *IEEE Trans. Microw. Theory Tech.*, vol. 38, no. 8, pp. 1053–1058, Aug. 1990.

[2] X. Yuan, D. R. Lynch, and J. W. Strohbehn, "Coupling of finite element and moment methods for electromagnetic scattering from inhomogeneous objects," *IEEE Trans. Antennas Propag.*, vol. 38, no. 3, pp. 386–393, Mar. 1990.

[3] J. M. Jin and J. L. Volakis, "A hybrid finite element method for scattering and radiation by microstrip patch antennas and arrays residing in a cavity," *IEEE Trans. Antennas Propag.*, vol. 39, no. 11, pp. 1598–1604, Nov. 1991.
[4] G. E. Antilla and N. G. Alexopoulos, "Scattering from complex three-dimensional geometries by a curvilinear hybrid finite-element-integral equation approach," *J. Opt. Soc. Amer. A*, vol. 11, pp. 1445–1457, Apr. 1994.
[5] A. J. Poggio and E. K. Miller, *Integral Equation Solution of Three Dimensional Scattering Problems*. Elmsford, NY: Permagon, 1973, ch. 4.
[6] Y. Chang and R. F. Harrington, "A surface formulation for characteristic modes of material bodies," *IEEE Trans. Antennas Propag.*, vol. 25, pp. 789–795, 1977.
[7] T. K. Wu and L. L. Tsai, "Scattering from arbitrarily-shaped lossy dielectric bodies of revolution," *Radio Sci.*, vol. 12, pp. 709–718, 1977.
[8] T. K. Sarkar, S. M. Rao, and A. R. Djordjević, "Electromagnetic scattering and radiation from finite microstrip structures," *IEEE Trans. Microwave Theory Tech.*, vol. 38, no. 11, pp. 1568–1575, Nov. 1990.
[9] S. M. Rao, C. C. Cha, R. L. Cravey, and D. L. Wilkes, "Electromagnetic scattering from arbitrary shaped conducting bodies coated with lossy materials of arbitrary thickness," *IEEE Trans. Antennas Propag.*, vol. 39, no. 5, pp. 627–631, May 1991.
[10] A. A. Kishk, A. W. Glisson, and P. M. Goggans, "Scattering from conductors with materials of arbitrary thickness," *IEEE Trans. Antennas Propag.*, vol. 40, no. 1, pp. 108–111, Jan. 1992.
[11] B. M. Kolundzija, "Electromagnetic modeling of composite metallic and dielectric structures," *IEEE Trans. Microwave Theory Tech.*, vol. 47, no. 7, pp. 1021–1032, Jul. 1999.
[12] L. N. Medgyesi-Mitschang, J. M. Putnam, and M. B. Gedera, "Generalized method of moments for three-dimensional penetrable scatterers," *J. Opt. Soc. Amer. A*, vol. 11, no. 4, pp. 1383–1398, Apr. 1994.
[13] M. Carr, E. Topsakal, and J. L. Volakis, "A procedure for modeling material junctions in 3-D surface integral equation approaches," *IEEE Trans. Antennas Propag.*, vol. 52, no. 5, pp. 1374–1379, May 2004.
[14] J. Shin, A. W. Glisson, and A. A. Kishk, "Generalization of surface junction modeling for composite objects in an SIE/MoM formulation using a systematic approach," *ACES J.*, vol. 20, no. 1, pp. 1–12, Mar. 2005.
[15] J. H. Richmond, "Scattering by a dielectric cylinder of arbitrary cross section shape," *IEEE Trans. Antennas Propag.*, vol. 13, no. 3, pp. 334–341, 1965.
[16] ——, "TE-wave scattering by a dilectric cylinder of arbitrary cross section shape," *IEEE Trans. Antennas Propag.*, vol. 14, no. 4, pp. 460–464, Jul. 1966.
[17] D. E. Livesay and K. M. Chen, "Electromagnetic fields inside arbitrarily shaped biological bodies," *IEEE Trans. Microwave Theory Tech.*, vol. 22, no. 12, pp. 1273–1280, Dec. 1974.
[18] D. H. Schaubert, D. R. Wilton, and A. W. Glisson, "A tetrahedral modeling method for electromagnetic scattering by arbitrary shaped inhomogeneous dielectric bodies," *IEEE Trans. Antennas Propag.*, vol. 32, no. 1, pp. 77–85, Jan. 1984.
[19] R. D. Graglia, D. R. Wilton, and A. F. Peterson, "High order interpolatory vector bases on prism elements," *IEEE Trans. Antennas Propag.*, vol. 46, pp. 442–450, Mar. 1998.
[20] R. D. Graglia, P. L. E. Uslenghi, and R. S. Zich, "Moment method with isoparametric elements for three-dimensional anisotropic scatterers," *Proc. Inst. Elect. Eng.*, vol. 77, no. 5, pp. 750–760, May 1989.
[21] W. C. Chew and C. C. Lu, "The use of Hyugen's equivalence principle for solving the volume integral equation of scattering," *IEEE Trans. Antennas Propag.*, vol. 41, no. 7, pp. 897–904, Jul. 1993.
[22] J. L. Volakis, "Alternative field representation and integral equations for modeling inhomogeneous dielectrics," *IEEE Trans. Microwave Theory Tech.*, vol. 40, no. 3, pp. 604–608, Mar. 1992.
[23] A. F. Peterson, "Application of volume discretization methods to oblique scattering from high-contrast penetrable cylinders," *IEEE Trans. Microwave Theory Tech.*, vol. 42, no. 4, pp. 686–689, Apr. 1994.
[24] J. P. Kottmann and O. J. F. Martin, "Accurate solution of the volume integral equation for high-permittivity scatterers," *IEEE Trans. Antennas Propag.*, vol. 48, no. 11, pp. 1710–1726, Nov. 2000.
[25] E. Bleszynski, M. Bleszynski, and T. Jaroszewicz, "An efficient integral equation based solution method for simulation of electromagnetic fields in inhomogeneous dielectric (biological) media," in *ACES Conference*, Monterey, CA, March 2000.
[26] J. M. Jin, J. L. Volakis, and V. V. Liepa, "A moment method solution of a volume-surface integral equation using isoparametric elements and point matching," *IEEE Trans. Microwave Theory Tech.*, vol. 37, no. 10, pp. 1641–1645, October 1989.
[27] R. C. Bauke and A. F. Peterson, "A new volume integral equation method for 2-D inhomogeneous composite structures using one unknown per node," *IEEE Trans. Magn.*, vol. 27, no. 5, pp. 4279–4282, Sep. 1991.
[28] T. Vaupel and V. Hansen, "Electrodynamic analysis of combined microstrip and coplanar/slotline structures with 3-D components based on a surface/volume integral-equation approach," *IEEE Trans. Microwave Theory Tech.*, vol. 47, no. 9, pp. 1788–1800, Sep. 1999.
[29] C. C. Lu and W. C. Chew, "A coupled surface-volume integral equation approach for the calculation of electromagnetic scattering from composite metallic and material targets," *IEEE Trans. Antennas Propag.*, vol. 48, no. 12, pp. 1866–1868, Dec. 2000.
[30] F. Tiezzi and R. Mosig, "Analysis of printed antenna with inhomogeneous dielectric bodies," in *Proc. IEEE Antennas Propagation Int. Symp.*, 2002, pp. 862–865.
[31] Z. Chen and Y. Xu, "The Petrov-Galerkin and iterated Petrov-Galerkin methods for second-kind integral equations," *SIAM J. Num. Anal.*, vol. 35, no. 1, pp. 406–434, Feb. 1998.
[32] B. C. Usner, K. Sertel, and J. L. Volakis, "Conformal Galerkin testing for VIE using parametric geometry," *Electron.Lett.*, vol. 40, no. 15, pp. 926–927, Jul. 2004.
[33] M. N. Vouvakis, S. C. Lee, K. Zhao, and J. F. Lee, "A symmetric FEMIE formulation with a single-level IE-QR algorithm for solving electromagnetic radiation and scattering problems," *IEEE Trans. Antennas Propag.*, vol. 52, no. 11, pp. 3060–3070, Nov. 2004.
[34] K. Sertel and J. L. Volakis, "Method of moments solution of volume integral equations using parametric geometry modeling," *Radio Sci.*, vol. 37, no. 1, pp. 101–107, 2002.
[35] P. L. Huddleston, L. N. Medgyesi-Mitschang, and J. M. Putnam, "Combined field integral equation formulation for scattering by dielectrically coated conducting bodies," *IEEE Trans. Antennas Propag.*, vol. 34, pp. 510–520, Apr. 1986.
[36] Z. Q. Zhang and Q. H. Liu, "Three-dimensional nonlinear image reconstruction for microwave biomedical imaging," *IEEE Trans. Biomed. Eng.*, vol. 51, no. 3, pp. 544–548, Mar. 2004.

Brian C. Usner (S'00) received the B.S. degree in electrical engineering from Tulane University, New Orleans, LA, in 2001, and the M.S. degree in electrical engineering from the University of Michigan, Ann Arbor, in 2002. He is currently working toward the Ph.D. degree in electrical engineering at The Ohio State University, Columbus.

He was a Departmental Fellow in the Electrical Engineering department at the University of Michigan. In addition, he was a University Fellow at the Ohio State University where he is currently a NASA GSRP Fellow working at the ElectroScience Laboratory. His research interests are in the areas of computational EM with emphasis on tool development for EM design.

Mr. Usner is also a member of the IEEE Antennas and Propagation Society.

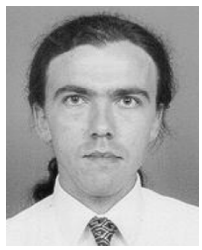

Kubilay Sertel (M'03) received the B.S. degree from Middle East Technical University, Ankara, Turkey, in 1995, the M.S. degree from Bilkent University, Ankara, Turkey, in 1997, and the Ph.D. degree from the electrical engineering and Computer Science Department, University of Michigan, Ann Arbor, in 2003.

He is currently a Senior Research Associate at the ElectroScience Laboratory, The Ohio State University, Columbus. His research areas include electromagnetic theory, computational electromagnetics, integral equation and hybrid methods, fast and efficient methods for large-scale electromagnetics problems and parallel implementations of fast algorithms.

Michael A. Carr (M'03) received the B.S. degree from Ohio Northern University, Ada, in 1996 and the M.S. and Ph.D. degrees from the University of Michigan at Ann Arbor, 1999 and 2002, respectively, all in electrical engineering.

Since January, 2003, he has been a Senior Research Associate with The Ohio State University, Columbus, where he continues his work with numerical electromagnetic techniques, including fast methods, preconditioners, material modeling, and hybrid techniques.

Dr. Carr is a member of IEEE, Tau Beta Pi, and Phi Eta Sigma. He is also a pilot.

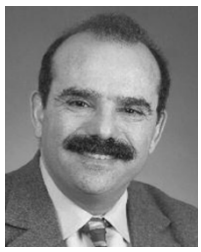

John L. Volakis (S'77–M'82–SM'89–F'96) was born on May 13, 1956, in Chios, Greece. He received the B.E. degree (*summa cum laude*) from Youngstown State University, Youngstown, OH, in 1978 and the M.Sc. and Ph.D. degrees The Ohio State University, Columbus, in 1979 and 1982, respectively.

From 1982 to 1984, he was with Rockwell International, Aircraft Division, Lakewood, CA, and during 1978 to 1982, he was a Graduate Research Associate at the ElectroScience Laboratory, The Ohio State University. From 1984 to 2002, he was a Professor in the Electrical Engineering and Computer Science Department, University of Michigan, Ann Arbor, where from 1998 to 2000, he also served as the Director of the Radiation Laboratory. Since January 2003, he has been the Roy and Lois Chope Chair Professor of Engineering at The Ohio State University, Columbus, and also serves as the Director of the ElectroScience Laboratory. He has published over 220 articles in major refereed journal articles (nine of these have appeared in reprint volumes), more than 250 conference papers and ten book chapters. In addition, he coauthored two books *Approximate Boundary Conditions in Electromagnetics* (London, U.K.: IEE, 1995) and *Finite Element Method for Electromagnetics* (New York: IEEE Press, 1998). From 1994 to 1997, he was an Associate Editor of *Radio Science* and is currently an Associate Editor for the *Journal of Electromagnetic Waves and Applications*. He has also written two well-edited coursepacks on introductory and advanced numerical methods for electromagnetics, and has delivered short courses on numerical methods, antennas and frequency selective surfaces. His primary research deals with computational methods, electromagnetic compatibility and interference, design of new RF materials, multiphysics engineering and bioelectromagnetics.

Dr. Volakis is a Member of Sigma Xi, Tau Beta Pi, Phi Kappa Phi, and Commissions B and E of the International Union of Radio Science (URSI). In 1998, he received the University of Michigan College of Engineering Research Excellence award and in 2001 he received the Department of Electrical Engineering and Computer Science Service Excellence Award. He graduated/mentored 40 Ph.D. students/postdoctorates, and coauthored with them five papers receiving best paper awards at conferences. He served as an Associate Editor of the IEEE TRANSACTIONS ON ANTENNAS AND PROPAGATION from 1988 to 1992, and is currently an Associate Editor for the IEEE ANTENNAS AND PROPAGATION SOCIETY MAGAZINE and the *URSI Bulletin*. He chaired the 1993 IEEE Antennas and Propagation Society Symposium and Radio Science Meeting, and was a Member of the AdCom for the IEEE Antennas and Propagation Society from 1995 to 1998. From 1994 to 1997 he served as the President of the IEEE Antennas and Propagation Society. He is listed by ISI among the top 250 most referenced authors (2004, 2005). He is also listed in several Who's Who directories, including *Who's Who in America*.